

# Conducting Polymer Composites of Multiwalled Carbon Nanotube Filled Doped Polyaniline

Faris Yılmaz,<sup>1</sup> Zuhale Küçükyavuz<sup>2</sup>

<sup>1</sup>Department of Polymer Science and Technology, Middle East Technical University, Ankara, Turkey

<sup>2</sup>Department of Chemistry, Middle East Technical University, Ankara, Turkey

Received 12 February 2008; accepted 18 June 2008

DOI 10.1002/app.29132

Published online 13 October 2008 in Wiley InterScience (www.interscience.wiley.com).

**ABSTRACT:** A multiwalled carbon nanotube (c-MWNT)/ polyaniline (PANI) composite was synthesized by an *in situ* chemical oxidative polymerization process. With the carbon nanotube loading increased from 0 to 30 wt %, the conductivity also increased and became weakly temperature-dependent. Fourier transform infrared spectroscopy studies showed that the synthesis by an *in situ* process led to effective site-selective interactions between the quinoid ring of the PANI and the multiwalled nanotubes, facilitating

charge-transfer processes between the two components. The morphological analysis indicated that the c-MWNTs were well dispersed and isolated, and the tubes became crowded proportionally to the weight percentage of c-MWNTs used in the composites. © 2008 Wiley Periodicals, Inc. *J Appl Polym Sci* 111: 680–684, 2009

**Key words:** conducting polymers; fillers; infrared spectroscopy; nanocomposites

## INTRODUCTION

Polyaniline (PANI), with its good processability, environmental stability, and reversible control of electrical properties by both charge-transfer doping and protonation, is a unique and promising candidate among various conducting polymers.<sup>1,2</sup>

Carbon nanotubes (CNTs) have excellent thermal stability and unique mechanical and electrical properties and are of great interest for developing classes of multifunctional materials.<sup>3</sup>

Composites of PANI and CNTs have been prepared and investigated by several researchers.<sup>4–12</sup> Almost all of the reported PANI/CNT composites have shown enhanced electronic and mechanical properties.

In this study, on the basis of the interaction between aniline monomers and multiwalled carbon nanotubes (c-MWNTs), we synthesized a nanotubular material of multiwalled CNTs coated with PANI by using an *in situ* chemical oxidative polymerization method. The effects of CNTs on the conductivity of CNT/PANI composites are discussed in detail.

## EXPERIMENTAL

Synthesis-grade aniline, ammonium persulfate [(NH<sub>4</sub>)<sub>2</sub>S<sub>2</sub>O<sub>8</sub>], and hydrochloric acid (HCl; 37%)

were purchased from Merck (Darmstadt, Germany). Aniline monomer was distilled and stored under 0°C before use. Multiwalled nanotubes (MWNTs), with an average diameter of 10 nm, a length of 0.1–10 μm, a Brunauer–Emmett–Teller (BET) surface area of 250–300 m<sup>2</sup>/g, a carbon purity of about 90%, and a metal oxide (impurity) content of about 10%, were purchased from Nanocyl S.A. (Hamburg, Germany).

A tubular composite of protonic acid doped PANI with c-MWNTs was synthesized by *in situ* chemical oxidative polymerization. In a typical experiment, a solution (150 mL) of 1M HCl, containing c-MWNTs, was sonicated at room temperature to disperse the CNTs. The aniline monomer (5 g, ~ 0.054 mol) was dissolved in 100 mL of 1M HCl and then added to the c-MWNT suspension. A solution of 1M HCl (50 mL) containing the oxidant (NH<sub>4</sub>)<sub>2</sub>S<sub>2</sub>O<sub>8</sub> (12.3 g, ~ 0.054 mol) was slowly added with constant sonication at a temperature of about 3°C to the mixture of aniline and MWNTs. After a few minutes, the dark suspension became green, and this indicated good polymerization of aniline; then, it was sonicated for 3 h at 3°C. The composite was obtained by filtration and rinsing of the suspension with 1M HCl followed by drying of the remaining powder *in vacuo* at room temperature for 24 h. In this process, PANI existed in its primary doped form, emeraldine salt (ES). Different composites were synthesized by this process with a 0, 5, 10, 15, or 30 wt % concentration of c-MWNTs (based on the weight of the monomer).

Fourier transform infrared (FTIR), X-ray diffraction, thermogravimetric analysis (TGA), scanning

Correspondence to: Z. Küçükyavuz (zuhale@metu.edu.tr).

electron microscopy (SEM), and direct-current conductivity were used to characterize the composite. FTIR spectra were taken with a Bruker IFS 66/S (Ettlingen, Germany) using the wave-number range of 450–4000  $\text{cm}^{-1}$ . The specimen for FTIR analysis was prepared by the grinding of a powdery sample with KBr powder (weight ratio  $\approx 1 : 99$ ) and then the pressing of the mixture into tablets. X-ray powder diffraction was carried out on a Rigaku Miniflex (The Woodlands, TX) using Cu  $K\alpha$  radiation and a scan angle ranging from 5 to 60° at a scanning rate of 1°/min and with a step size of 0.05°. TGA (Pyris 1, PerkinElmer, Waltham, MA) was conducted to measure the weight loss of the composite powder from room temperature to 1000°C at a heating rate of 10°C/min under a nitrogen stream. The four-probe measurement of conductivity based on van der Pauw's theorem<sup>13</sup> was used. Composite samples were pressed into tablets, and the conductivity was determined with a Keithley 614 electrometer (Cleveland, OH). The tubular morphology of the composite was observed with SEM (model JSM-6400, JEOL (Peabody, MA); low voltage of 20 kV).

## RESULTS AND DISCUSSION

The formation of tubular composites is believed to arise from the strong interaction between the aniline monomer and MWNTs. The interaction possibly comes from the  $\pi$ - $\pi$  electron interaction between MWNTs and the aniline monomer. Such a strong interaction ensures that the aniline monomer is adsorbed onto the surface of MWNTs during the formation of tubular composites. MWNTs, therefore, serve as the template and the core during the formation of tubular composites. Because of the random formation of MWNT bundles, there are some special gaps between individual MWNTs. Aniline molecules are wedged into such special gaps because of the strong interaction between the MWNTs and aniline monomer and then *in situ* polymerization. As the polymerization proceeds, the growing PANI macromolecules break down the CNT bundles into individual CNTs, and thus MWNTs can be dispersed into PANI matrices uniformly and individually. Because of the site-selective interaction between the quinoid ring of the polymer and MWNTs, PANI macromolecules are also adsorbed at the surface of the MWNTs and form the shell of tubular composites.<sup>4,10</sup> Another mechanism of composite formation<sup>14</sup> can be explained as follows: When CNTs are dispersed in an aniline/HCl solution, aniline hydrochloride ions are adsorbed onto the nanotube surface. Upon the addition of the oxidant  $[(\text{NH}_4)_2\text{S}_2\text{O}_8]$ , the adsorbed species are oxidized and form cation radicals, which initiate polymerization on the surface. The reaction takes place faster on the surface of

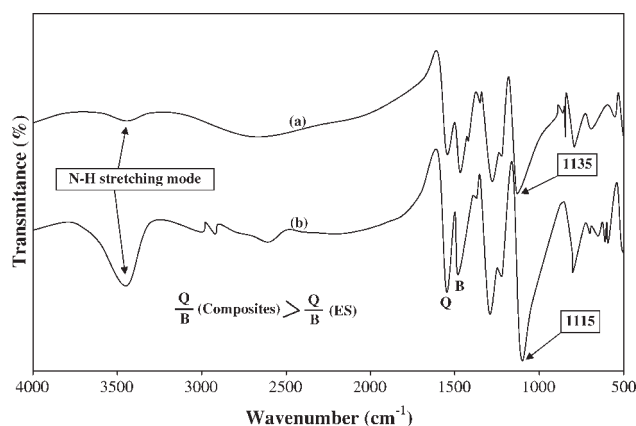
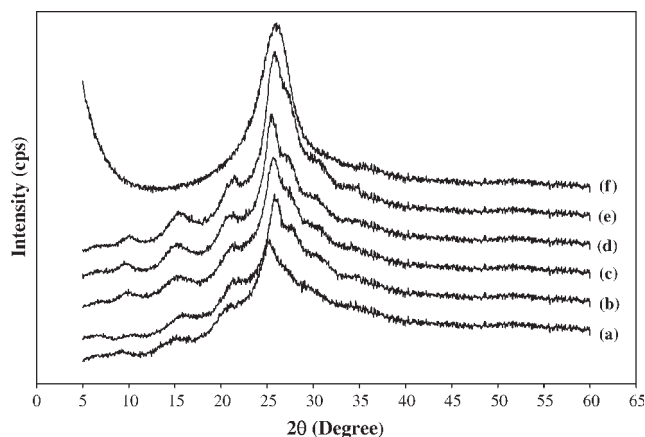


**Figure 1** FTIR spectra of the (a) ES PANI form and (b) 15 wt % MWNT-PANI ES composite.

CNTs than in the bulk because of the low activation energy (based on the principles of heterogeneous catalysis). This leads to the formation of the PANI shell over CNTs. Thus, the nanotubes act as a template for the formation of tubular composites. In a well-dispersed solution of CNTs, the adsorption of aniline hydrochloride will be high and uniform, and this can lead to the formation of a thicker uniform coating of PANI.

Figure 1 shows the FTIR spectra for doped PANI and a doped *in situ* prepared composite (this spectrum is very similar to the FTIR spectra found in ref. 15). The two spectra exhibit the clear presence of benzenoid and quinoid ring vibrations at 1500 and 1600  $\text{cm}^{-1}$ , respectively, indicating the oxidation state of ES PANI.<sup>15</sup> The quinoid band at 1600  $\text{cm}^{-1}$  for ES PANI is less intense than that of the benzenoid band at 1500  $\text{cm}^{-1}$ . The N—H stretching mode is shown by a very weak and broad band near 3400  $\text{cm}^{-1}$ . The strong band at 1150  $\text{cm}^{-1}$  is a characteristic of the so-called electronic-like band described by MacDiarmid et al.,<sup>15</sup> which is a measure of the degree of delocalization of the electrons and thus a characteristic peak of PANI conductivity. In Figure 1, there are several differences between the composite spectrum and pure ES PANI spectrum. The composite spectrum exhibits an inverse 1600/1500  $\text{cm}^{-1}$  intensity ratio compared to that of the ES without CNTs, and this indicates that the PANI in the composite is richer in quinoid units than the pure ES PANI. This may suggest that nanotube/PANI interactions promote and/or stabilize the quinoid ring structure. Also, a difference between the two spectra can be found in the N—H stretching region near 3400  $\text{cm}^{-1}$ . It is broad and strong in the composite samples and very weak in the spectrum of pure ES PANI.

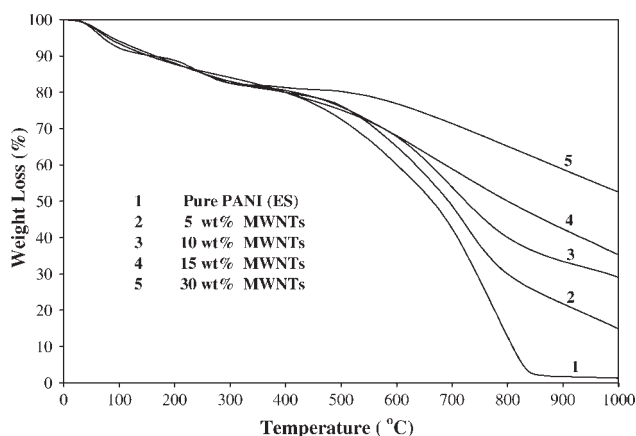
The intensity of other peaks in the composite spectrum is increased and shifted with respect to the peaks observed for the pure ES form. For example, the intensity of the signal at 1135  $\text{cm}^{-1}$  increases and



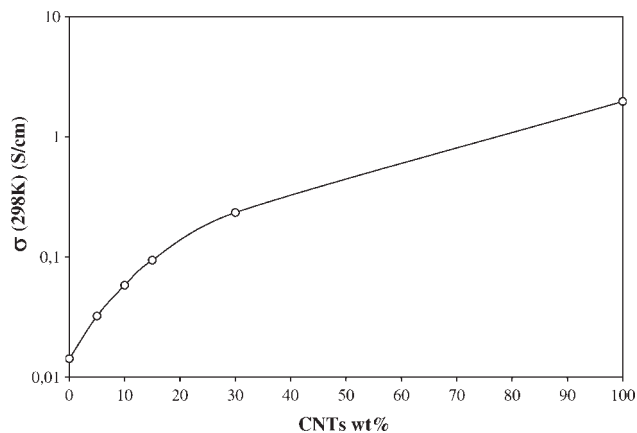
**Figure 2** X-ray diffractograms (Cu  $K\alpha$ ) of the (a) doped PANI ES type; composites containing (b) 5, (c) 10, (d) 15, and (e) 30 wt % MWNTs; and (f) MWNTs.

shifts to  $1115\text{ cm}^{-1}$ . This dramatic increase in the designated electronic-like absorption peak (defined as  $-\text{N}=\text{quinoid}=\text{N}-$ ) agrees well with our increased conductivity measurements. It appears that the interaction between PANI and MWNTs increases the effective degree of electron delocalization and thus enhances the conductivity of the polymer chains. The strong interaction may result in the functioning of CNTs as chemical dopants for PANI conductivity.<sup>15</sup>

The structural characteristics of the composite and its constituents have been analyzed by X-ray powder diffraction measurements and are shown in Figure 2. At lower angles, the diffractograms of the PANI/MWNT materials show the highly pronounced oscillating structure of the primary doped PANI (ES) with an oxidation degree of 0.5, and at higher angles, they superimposed the typical MWNT peaks, whose heights increase proportionally to their weight percentage. Therefore, it is clear that from a structural point of view no additional order has been introduced.



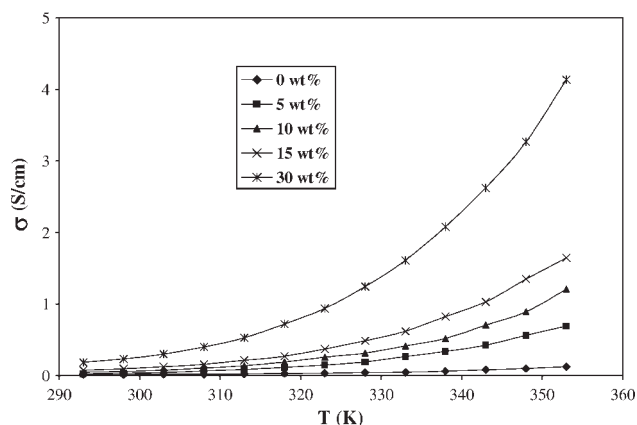
**Figure 3** Thermogravimetric behavior of pure PANI (ES) and PANI/MWNT composites.



**Figure 4** Semilogarithmic plot of the room-temperature conductivity ( $\sigma$ ) of the composite versus the MWNT loading.

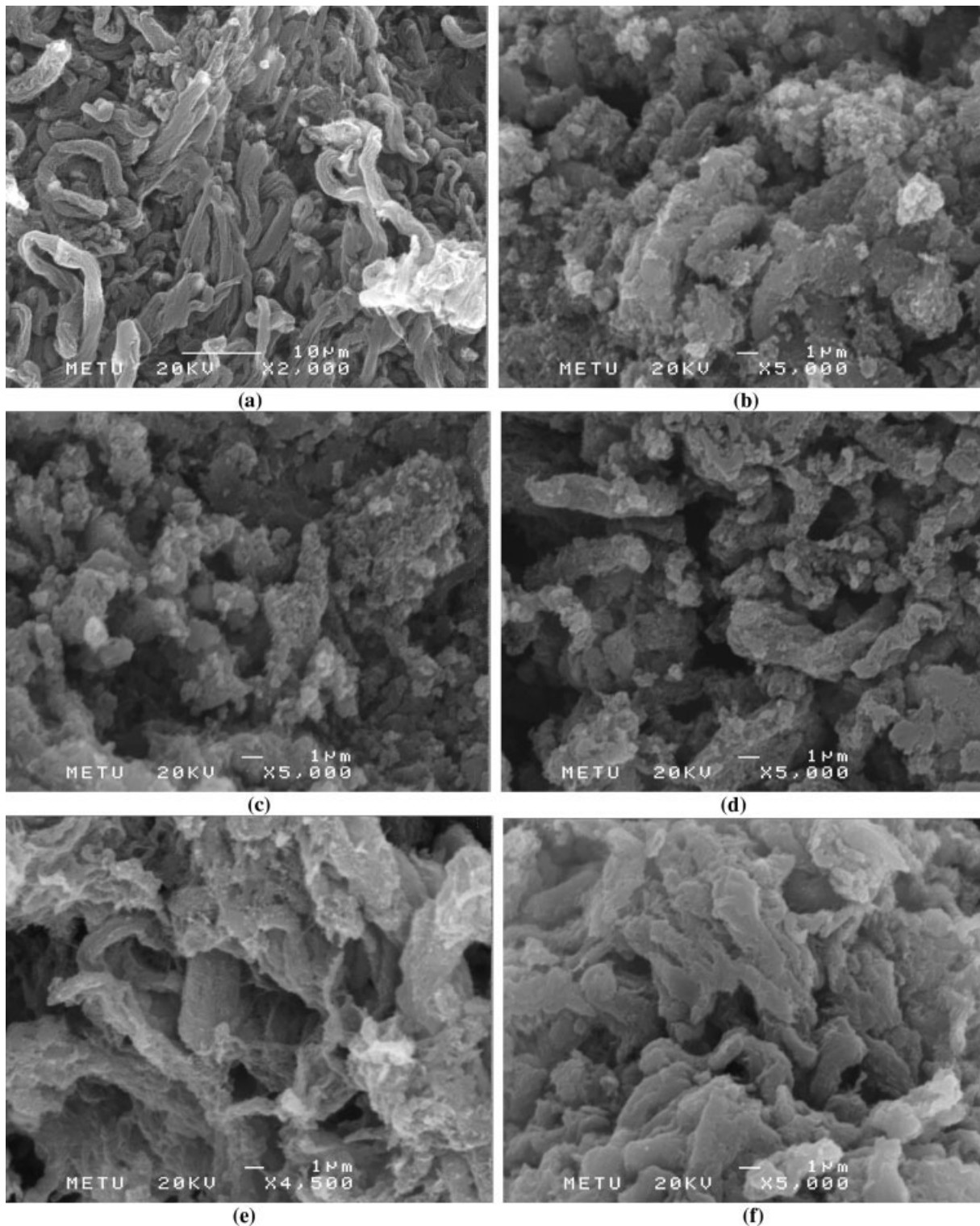
Figure 3 shows the TGA results for MWNT/PANI composite powders. This figure presents a typical three-step weight-loss behavior. In the first step, approximately 8% weight loss at temperatures up to  $130^\circ\text{C}$  can be seen. This can be attributed to a loss of water molecules from the composite structure. The second weight loss of about 2–3% at temperatures in the range of  $150\text{--}250^\circ\text{C}$  may possibly be due to the coevolution of water and evolution of acid. The third step starts at  $350^\circ\text{C}$  and represents the oxidative degradation of the composites; it also indicates the chemical structure decomposition of the composites. Moreover, by comparing the thermal behavior of composites containing different compositions of MWNTs, as shown in Figure 3, one can observe that MWNTs as fillers introduce higher thermal stability into the composite material.

Figure 4 shows the room-temperature conductivity of MWNT/PANI composites as a function of the MWNT loading. The conductivity of the pure PANI and MWNT is  $1.4 \times 10^{-2}$  and  $1.97\text{ S/cm}$ , respectively. Up to 15 wt %, the conductivity of the



**Figure 5** Temperature ( $T$ ) dependence on the conductivity of the composites.





**Figure 6** SEM image of (a) pure MWNTs and (b) 5, (c) 10, (d) 15, and (e,f) 30 wt % MWNT/PANI composites.

composites increases rapidly with an increase in the MWNT loading. For the 30 wt % composite, the conductivity is  $2.3 \times 10^{-1}$  S/cm, and this increases by 1 order of magnitude with respect to PANI. At higher concentrations, the increase in the conductivity will plateau; that is, the curve asymp-

totically will reach toward pure nanotubes ( $1.97$  S/cm). Here, we note that in many published articles<sup>16</sup> the loading of nanotubes is small ( $<5\%$ ), whereas the conductivity becomes saturated; this is possibly due to highly conductive CNTs ( $5.1 \times 10^4$  S/cm).<sup>16</sup>

To explore how the MWNTs affect the composite's conductivity, we measured the temperature dependence of the conductivity, as shown in Figure 5. The temperature dependence of the conductivity becomes weaker and weaker with the MWNT loading increasing. In this composite system, both the matrix (PANI) and the filler (MWNTs) are conducting. At high temperatures, conductivity is obtained by the polymer. With the temperature decreasing, the matrix becomes more and more resistive. On the other hand, the filler network, which shows very weak temperature dependence, becomes more conducting than the matrix at a low temperature. This means that the low-temperature conductivity is due to the MWNTs. A polymer composite with MWNTs can distinctly enhance the electronic properties of the polymer and even the MWNTs. For example, it has been reported that the conductivity of PANI/MWNT composites is higher than that of pressed MWNTs (or PANI).<sup>10,17</sup> A possible reason is the fact that there is some interaction between the MWNTs and the polymer chains. However, the nature of this interaction is not very clear yet. Maser et al.<sup>10</sup> pointed out that synthesis by an *in situ* process leads to effective site-selective interactions between the quinoid ring of PANI and MWNTs, and this facilitates charge-transfer processes between the two components.

The morphology and size of the composites were analyzed by SEM in detail. Figure 6(a) shows a typical SEM image of pure MWNTs. The MWNTs are very long and highly entangled in the solid state to form a dense, robust, network structure. It is very difficult for the MWNTs to be well dispersed in the polymer matrix. The diameters of the MWNTs are in the range of 10–15 nm.

SEM images of the composite with 30 wt % MWNTs are given in Figure 6(e,f). Microscopy studies have shown a tubular-type morphology for the composite, which has a core-shell structure,<sup>18</sup> the CNTs being the cores encapsulated by a PANI shell. Also, SEM images of the composites containing 5, 10, or 15 wt % MWNTs are presented in Figure 6(b–d), respectively. Compared to the CNT diameters, the diameters in the tubular composite are high. The microscopy images show that in the composites, the nanotubes are uniformly and thickly coated with PANI. The tubes are almost uniform in diameter in the range of 90–105 nm. Moreover, the tubes in the composites become crowded proportionally to the weight percentage of MWNTs used in the composites.

## CONCLUSIONS

The composites exhibited an order of magnitude increase in electrical conductivity with an increase in the CNT content over neat PANI and became weakly temperature dependent. The measured

increase in the conductivity of the composites may have been due to a doping effect of CNTs in which the nanotubes competed with chloride ions. Infrared spectroscopy showed that the synthesis by an *in situ* process led to effective site-selective interactions between the quinoid ring of PANI and MWNTs, facilitating charge-transfer processes between the two components. Moreover, MWNTs affected both the free N–H environment and quinoid units along the polymer backbone and perhaps were responsible for the strong interactions between the nanotubes and PANI. Wide-angle X-ray diffraction showed a highly pronounced oscillating structure of the primary doped PANI ES at lower angles and superimposed the typical MWNT peaks at higher angles; therefore, no additional order was introduced. TGA indicated three-step weight-loss behavior at 130°C, between 150 and 250°C, and at 350°C, demonstrating the loss of water, coevolution of water or evolution of acid, and decomposition of the composite backbone, respectively. Also, MWNTs as fillers introduced higher thermal stability into the composites. Finally, SEM measurements indicated that the MWNTs were well dispersed and isolated, and the tubes became crowded proportionally to the weight percentage of MWNTs used in the composites.

## References

1. Skotheim, T. A.; Elsenbaumer, R. L.; Reynolds, J. R. *Handbook of Conducting Polymers*; Marcel Dekker: New York, 1997.
2. Premamoy, G.; Samir, K. S.; Amit, C. *Eur Polym J* 1999, 35, 699.
3. Zhou, Y.; He, B.; Zhou, W.; Huang, J.; Li, X.; Wu, B.; Li, H. *Electrochim Acta* 2004, 49, 257.
4. Zhang, X.; Zhang, J.; Liu, Z. *Appl Phys A* 2005, 80, 1813.
5. Blanchet, G. B.; Fincher, C. R.; Gao, F. *Appl Phys Lett* 2003, 82, 1290.
6. Ramamurthy, P. C.; Harrell, W. R.; Crecory, R. V.; Sadandan, B.; Rao, A. M. *Polym Eng Sci* 2004, 44, 28.
7. Choi, H. J.; Park, S. J.; Kim, S. T.; Jhon, M. S. *Diamond Relat Mater* 2005, 14, 766.
8. Maser, W. K.; Benito, A. M.; Callejas, M. A.; Seeger, T.; Martinez, M. T.; Schreiber, J.; Chanvet, O.; Biro, L. P. *Mater Sci Eng C* 2003, 23, 87.
9. Huang, J. E.; Li, X. H.; Xu, J. C.; Li, H. L. *Carbon* 2003, 41, 2731.
10. Cochet, M.; Maser, W. K.; Chauvet, O. *Chem Commun* 2001, 1450.
11. Long, Y.; Chen, Z.; Liu, Z. *Appl Phys Lett* 2004, 85, 1796.
12. Liu, J.; Tian, S.; Knoll, W. *Langmuir* 2005, 21, 5596.
13. van der Pauw, L. J. *Philips Res Rep* 1958, 13, 1.
14. Philip, B.; Xie, J.; Abraham, J. K.; Varadan, V. K. *Polym Bull* 2005, 52, 127.
15. Zengin, H.; Zhou, W.; Jin, J.; Czerw, R.; Smith, D. W., Jr.; Echegoyen, L.; Carroll, D. L.; Foulger, S. H.; Ballato, J. *Adv Mater* 2002, 14, 1480 and references therein.
16. Ramasubramaniam, R.; Chen, J.; Liu, H. Y. *Appl Phys Lett* 2003, 83, 2928.
17. Shlovskii, B. I.; Efros, A. L. *Electronic Properties of Doped Semiconductors*; Springer: Berlin, 1984.
18. Philip, B.; Xie, J.; Abraham, J. K.; Varadan, V. K. *Smart Mater Struct* 2004, 13, 105.